ADVANCED COMPUTATIONAL TECHNIQUES FOR THE EVALUATION OF SOLAR ACTIVITIES

Abstract

In this work, we examined more advanced methods of data processing; specifically, we used wavelet approaches to identify several properties of the Sun, such as sunspots, solar winds, interplanetary magnetic field components (IMF), so on. In order to conduct an analysis of the astronomical and solar data, one can make use of a number of different mathematical transformations. Among them, the Fourier transform is one of the most used and well-known methods. In situations where higher performance is desired, the Wavelet Transform is used to get beyond the constraints it places on the system because it has some limits. Within the span of a decade, numerous academics working in a variety of scientific fields made use of this methodology. As a result of its exceptional performance, faultless operation, and ready availability, it will become more helpful and well-known among new researchers as they develop their original concepts.

Keywords: Space Weather, Sun’s parameters, Wavelet Techniques

Authors

Satish Kumar Kasde
Department of Physics
Government College Bhainsdehi
Betul**,** Madhya Pradesh, India
sbskasde@gmai.com

D.K. Sondhiya
School of Sciences
SAGE University Bhopal, India

I. INTRODUCTION

All space weather on or near Earth originates from the Sun. Convective motion under the solar surface causes sunspots. The nature and characteristics of the solar wind can be better understood through changes in its parameters. Multifractality and intermittency phenomena distinguish these variants. Space weather occurs when the Earth's magnetosphere interacts with solar particles and magnetic fields. Particles in the form of solar wind are ejected from the sun during solar flares and coronal mass ejections. Figure (1) depicts how space weather could endanger human life and health, as well as disrupt the operation of technological devices both on Earth and in space. Sun is responsible for Earth's space weather. Interplanetary magnetic field variations, solar CMEs, and Earth's magnetic field are all examples of space weather [1, 2]. A solar magnetic field and sunspots share a strong connection. Sunspots are produced by convective motion close to the solar surface. The Sun's magnetic field is transported to the planets by solar wind (IMF). Because it is a gaseous mass, the Sun revolves unevenly, with the equator spinning slightly faster (24–27 days) than the poles (30–35 days). Numerous techniques, such as correlation analysis [3, 4], chaos analysis [5, 6], multifractality analysis, have surely been used to study sunspots and related activities [7- 9]. Recently, multifractal analysis and chaos theory were applied to examine the statistical characteristics of solar activity [5]. The north-south asymmetries and rotational behavior of solar activity were examined using the wavelet and auto-correlation functions [3]. Studies have looked at cross-correlations between monthly mean sunspot areas and sunspot numbers [3]. When the magnetic, temperature, and density fields are all augmented, the F10.7cm radio flux (2800MHz) is utilized to measure overall solar activity[10].

In this chapter, we covered some of the most fundamental and significant characteristics of the sun. Several researchers account for all research parameters when conducting their research using established procedures and theories On the other hand, during the course of this chapter, we will present some sophisticated nonlinear approaches that can be used to a dataset of the Sun's parameters. Researchers throughout the world have been increasingly turning to non-linear methods in recent years in order to expand upon their previous work.

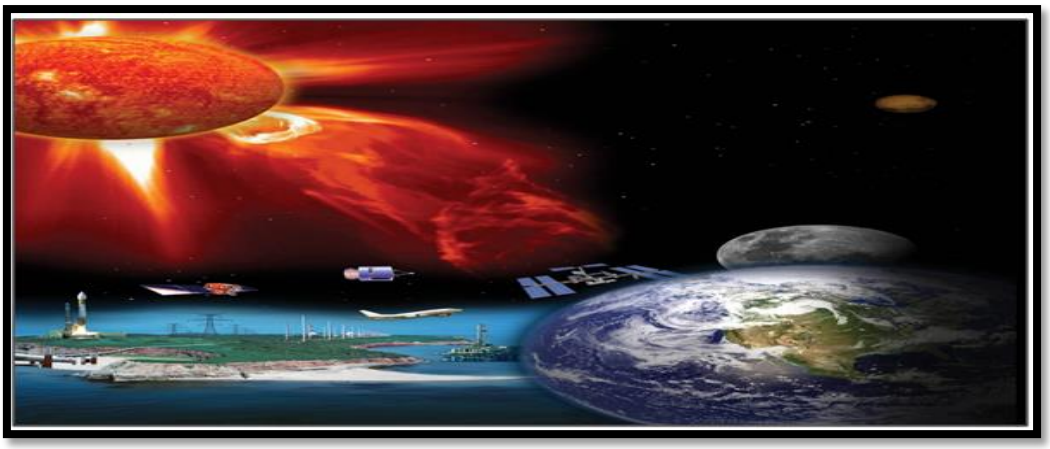

Courtesy: from NASA website

Figure 1: Space Weather and Earth's Atmosphere

II. STRUCTURE OF THE SUN

Figure (2) shows the Sun's regular shape. The Sun's core reaches 13 MK. Temperature and density allow nuclear fusion. Radioactivity surrounds the core. It takes photons produced deep within the core 106 years to travel to the outer atmosphere. Large-scale convective cells carry energy in the convective zone, which surrounds the radiation zone, driven by the temperature difference between the core and exterior of the sun. The photosphere is the outermost layer of the solar atmosphere. Chromospheres, transition zones, and coronas are all parts of the solar atmosphere. The following sections describe the Sun's components.

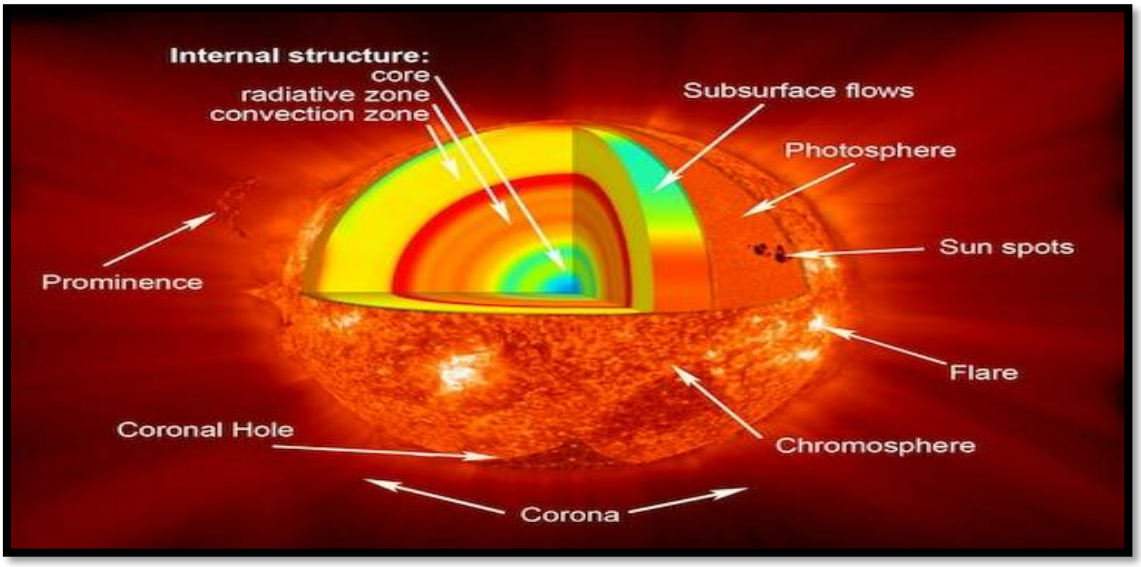

Courtesy: from NASA website

Figure 2: Sun's Standard Model

III. RADIATION ZONE

Energy is transferred from the extremely heated interior to the colder outer layers through photons. It contains the core. Due to the large concentrations in the core and radiation zone, P-P chain gamma rays scatter when they hit unbound electrons, protons, and atomic nuclei. These values vary from 10 to 5 MK and 0.25 to 0.75 R. Scattering occurs when an electron is entirely free (Thompson), weakly bound (Compton), or when the wavelength is substantially bigger than the atom (Rayleigh). When a bound electron absorbs a photon, bound-bound scattering occurs, moving the electron to a less bound state and causing stellar spectral absorption lines. In bound-free absorption, the absorbed photon's energy frees the electron and ionises the atom. The kinetic energy of an unbound electron near an ion increases during free-free absorption. Absorption prevails in the solar interior. Kramers' asserts that when bound-free and free-free absorption, T (-7/2) increases fast with decreasing temperature, lowering radiative transfer and steepening the temperature gradient.

IV. ATMOSPHERIC LAYERS OF THE SUN

Sun's inner part (i.e. core) to its outer layers of atmosphere is the source of its energy. As was discussed in the prior part of this chapter, an enormous amount of energy is carried from the Sun's core to the convection zone via the radiation zone. The following sections offer a concise introduction to the numerous phenomena that are related with the Sun's atmosphere and provide an overview of the Sun's atmosphere.

V. THE VISIBLE SURFACE (PHOTOSPHERE)

The word "photosphere" refers to the visible portion of the Sun, where the optical depth of light is unity. It is also sometimes referred to as the solar surface of final scattering for optical photons. The temperature at the bottom is around, while at the top, which is about above the "temperature minimum". Bubbles of hotter material that erupt from the sun and dissipate in a few minutes split the photosphere into sparkling grains. Magnetic field bundles can occasionally burst through the photosphere, disrupting this boiling layer with a combination of circumstances referred to as solar activity and creating cool and dark regions known as sunspots.

VI. THE CHROMOSPHERE (THE RED LAYER)

Above the photosphere is the chromosphere. Its 1500 km thick and hotter than the photosphere (compared to the photosphere, which is 5800 K, it is about 10000 K). As one moves higher into the chromospheres, the plasma density decreases and the amount of light emitted decreases proportionally. In some cases, the chromospheres are extremely active, with hot gas jets (spicules) shooting far into space. These can travel at speeds between 20 and 100 km/h and stretch thousands of kilometres above the solar surface. Since, the temperature in the chromosphere rises at a rate proportional to height squared, the chromosphere is relatively hot at great altitudes. Around their peripheries, you may spot solar prominences and spicules. The prominences, or solar filaments, that can be seen above the solar limb often take on a loop shape.

VII. THE SUN'S CROWN (CORONA)

The solar corona is the name given to the Sun's outer atmosphere during a solar eclipse. The corona, which means "crown" in Latin, expands supersonically into space. The term "solar wind" refers to the solar gas that escapes into planetary space. Not all directions of the corona are equally luminous or spherically symmetric. Since the corona is one million times fainter than the visible photosphere, it can only be viewed when the photographic plate is obscured. The three zones that make up the solar corona—active regions, calm sun regions, and coronal holes—all have different sizes depending on the stage of the sun's cycle.

1. **Active regions:** Active zones can be found where there are strong magnetic field concentrations, which can be visible as sunspot groups at optical wavelengths or magnetograms. The bulk of active zones are composed of closed magnetic field lines because of their bipolar nature. Persistent magnetic activity causes a number of dynamic processes in active regions, such as plasma heating, flares, and coronal mass ejections. These processes are caused by magnetic flux emergence, flux cancellation, magnetic reconfiguration, and magnetic reconnection. Active zones are often located within a

latitude range of 40 degrees from the solar equator. Sunspots, often referred to as active zones, first develop near 40 degrees of the solar equator and have the potential to cover 1% of the solar disc [11]. The umbra and penumbra of a sunspot are its lighter surrounding region and its black interior, respectively. In plain sunspots, the penumbra is made up of finer filaments that abruptly diverge from the umbra.

2. **Quiet Sun:** The areas that were left over outside of the active regions were designated as Quiet Sun regions. Because multiple dynamic processes have been discovered everywhere around the solar surface, the term "quiet Sun" is now considered to be an inaccurate misnomer. This is justified in comparison to other stars. In the calm sun, examples of dynamic processes include small-scale phenomena such as network heating events, nano-flares, explosive events, dazzling points, and soft X-ray jets. These phenomena occur on a very small scale. Examples of dynamic activities in the sun's calm surface include the formation of large-scale structures such as trans-equatorial loops and coronal arches. The boundary that divides active regions and quiet sun regions becomes increasingly fuzzy as a result of the majority of the large-scale structures that encompass quiet sun regions being anchored in active regions.

3. **Coronal holes:** During solar eclipses, it has been observed that the polar regions of the celestial globe are typically darker than the equatorial regions. As a result, Max Waldmeier named these regions "Koronale L'ocher" (in German, i.e., coronal holes). If there are any chromospheric upflows at their foot points, the open magnetic field lines that dominate these zones serve as effective conduits for flushing heated plasma from the corona into the solar wind. Coronal holes frequently lack plasma due to transport mechanisms, giving them a darker appearance than the calm Sun, where heated plasma streaming from the chromosphere is imprisoned until it cools and precipitates back to the chromosphere. Similar to how the atmosphere of our planet has a wide variety of cloud types, from dense stratocumulus to finely structured cirrus clouds, the solar corona also has a variety of loop morphologies that can provide crucial information about the magnetic reconnection and reconfiguration processes that are occurring underneath. While circular geometries may denote relaxed, near-dipolar magnetic field geometries, pointed and cusp-shaped structures may identify coronal null sites of X-type magnetic reconnection spots.

Solar Flares

Courtesy: from NASA website

Figure 3: Solar Flare and Coronal Mass Ejection

Solar flares in the solar atmosphere are responsible for the abrupt brightening of sunspot groupings (active regions). Richard Carrington was the one who made the initial discovery of solar flares in 1859. Solar flares are caused by the sudden release of magnetic energy that has been stored in the corona of the sun. According to this theory, the corona is the location where the energy is lighted, and the stronger a flare is, the deeper into the layer it can penetrate. Solar flares can be classified as either A, B, C, M, or X depending on their energy levels by looking at the peak flux (W/m2) of picometer X-rays near Earth, which is measured by the GOES spacecraft. As a result of the plasma heating, the solar flares cause charged particles (electrons, protons, and heavier ions) to accelerate to speeds that are very close to the speed of light. They generate electromagnetic radiation that extends across the entire electromagnetic spectrum, from radio waves to the shortest gamma rays, and everything in between. Solar flares and the associated coronal mass ejections (CMEs) seen in Figure [3] have a considerable influence on the space weather in our region locally. Radars and other pieces of equipment that operate on decimetric wavelengths have the potential to skew their direction. Solar flares are actually solar wind, which are incredibly powerful particles that can pose radiation risks for astronauts, spacecraft, and the magnetosphere of Earth. Solar flares can also generate solar prominences, which are bright spots on the sun.

Prominences

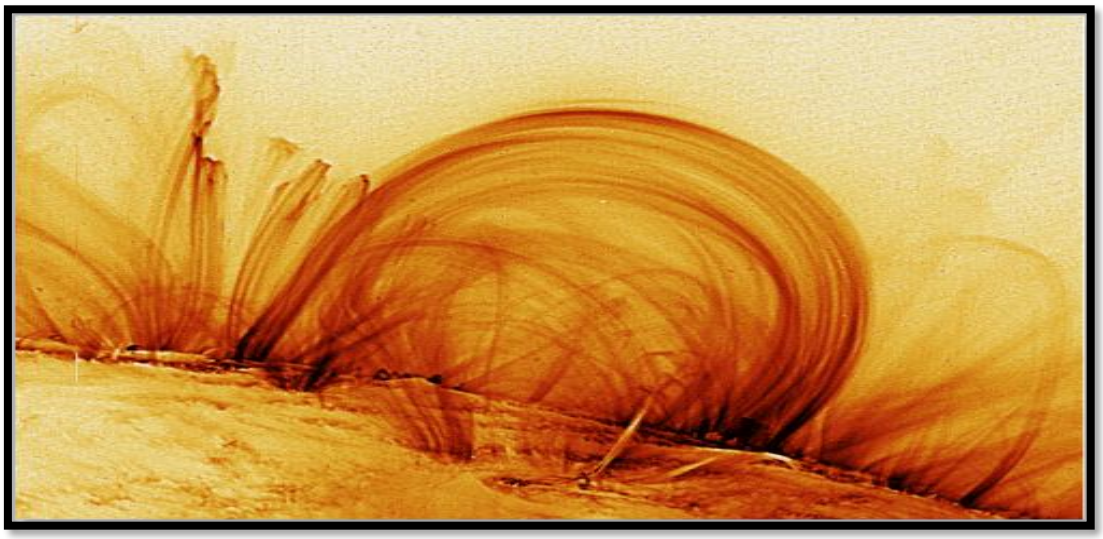

Courtesy: from NASA website

Figure 4: Prominences are Greatest Magnetic "Entity" of the Sun

Figure 4 depicts one of the greatest magnetic "entities" of Sun. Prominences are normally found during total solar eclipses and are described as "burning holes" or "red flames" [13], but before the 19th century some observations were made. In the 1870s, Angelo Secchi was the first to distinguish the prominences between quiescent and eruptive prominences, as depicted in Figure (5), [14].

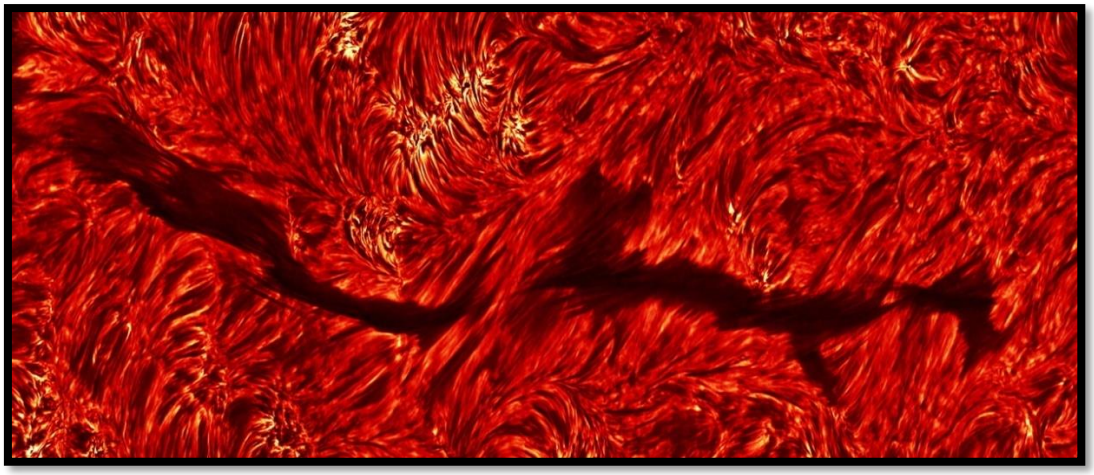

Courtesy: Dutch open Telescope (DOT), www.staff.science.uu.nl

Figure 5: Sun Showing Quiescent Prominence (Filament) the Full Length of Filament Taken in Halpha on October 6, 2004.

Quiescent prominences are a sun attraction. They originate in a day, remain "unchanged" for a month, and then end through CME eruptions (CMEs). Prominences in the solar corona consist of chromosphere-like plasma. Quiescent prominences have a length of $60 - 600\ Mm$, with a width of 5 to 15 Mm, its temperature varies from 4300 to 5500 K. It has average electron density of 10^{10} to $10^{11}\ cm^{-3}$, and pressure of 0.1 to 1 dyn/cm^2 with magnetic field strength of 4 to $20\,G$ [15-17]. There internal motions have a speed below10 km/s.

VIII. CORONAL MASS EJECTIONS

Coronal mass ejections(CME) are solar eruptions of mass and magnetic field from Sun. R. Tousey initially observed CMEs on December 14, 1971 with the 7th Orbiting Solar Observatory (OSO-7). LASCO on SOHO has been tracking CMEs since 1995. SOHO/LASCO measurements put the average speed of CMEs between 20 and 27,000 km/h (-1). CMEs have caused auroras on Earth's magnetosphere for thousands of years. Figure 6 demonstrates how CME affects Earth's magnetosphere.

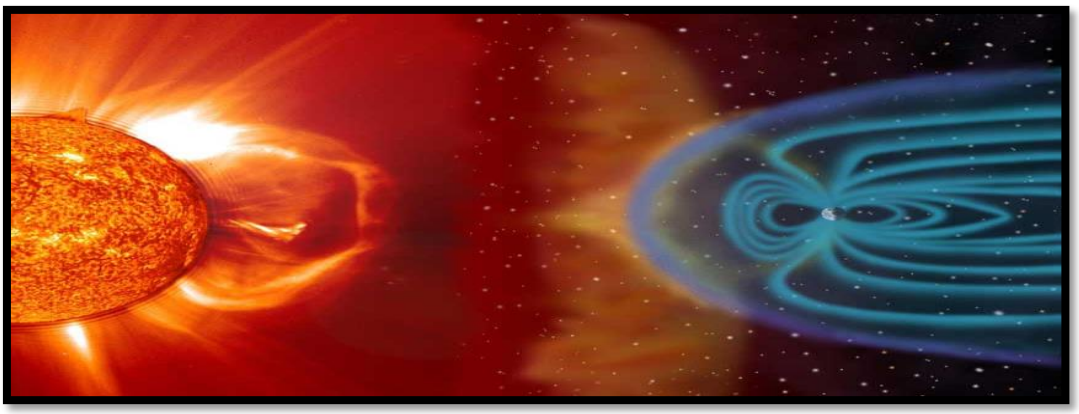

Courtesy: from NASA website

Figure 6: CME Interaction with Earth's Atmosphere.

IX. THE SOLAR CYCLE

Schwabe proposed that sunspots appear in quasi-periodic patterns of roughly 11 years [18].

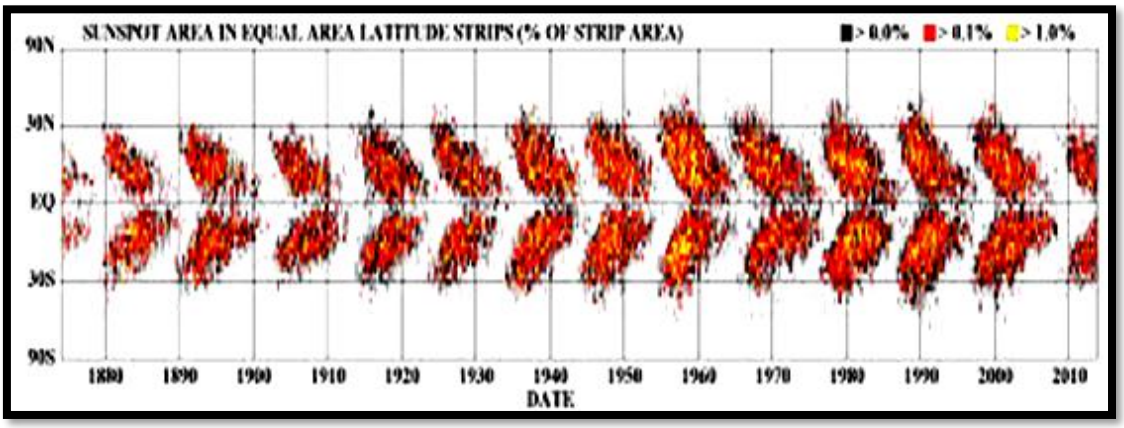

Courtesy: NASA Marshall Space Flight Center

Figure 7: The Sunspot Butterfly Diagram.

The life of a sunspot is generally short, ranging from days - weeks, and they begin to develop about mid-latitudes (approximately 30-400) on both hemispheres (Southern and Northern). As time passes, fresh sunspots appear closer and closer to the equator, as seen in Figure (7). The cyclic pattern of Solar activity from 1749-2000 was illustrated in Figure (8). It is divided in the period of Dolton minimum, End of Little Ice Age and Modern Warm Period that is current Solar cycle 24. Over an 11-year period known as the Solar Cycle, the Sun's number of sunspots varies. The Sun's activity and fluctuation are also described by the solar cycle. Sunspots typically last between one to one hundred days, while their total number varies over the course of this 11-year cycle. Sunspots are regions with strong magnetic fields, therefore fluctuations in their number indicate changes in the magnetic field of the Sun. The magnetic field of the Sun is similar to a dipole magnetic field during the Solar Minimum, with the magnetic field originating from one hemisphere and entering the other. The nice dipole arrangement eventually disappears as the Sun reaches solar maximum in the ensuing five to six years, and the Sun transforms into a very complicated, magnetically disordered object.

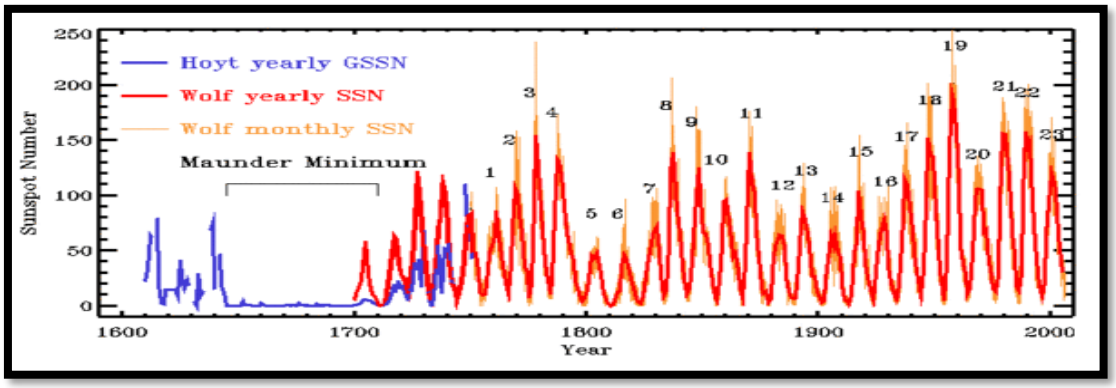

Courtesy: from NASA website

Figure 8: Long Term Sunspot Number Variations form 1600 to 2000

Five to six years later, when the sun reaches its maximum, the magnetic field re-organizes and becomes more dipolar. The orientation of the weak dipole field with respect to the Sun's spin axis is often rather tilted during this transition, but as solar minimum approaches, the dipole axis orientation gradually aligns with the spin axis. Reconstruct the dipole field with the polarity in the opposite direction from the original. This reversal in magnetic polarity is a defining feature of the Sun's 22-year magnetic cycle, which goes by a number of other names as well, including the double Solar cycle and the Hale cycle.

The polarity of pairs of sunspots also oscillates in this way. During the first 11 years of the magnetic cycle, the leading spots of each hemisphere always have the same polarity, which is always the complete opposite of the polarity of the other hemisphere's leading spot. For the next 11 years, sunspot polarity will be backwards. It stands to reason that the frequency of solar disturbances with an impact on Earth would mirror the sunspot or solar cycle, given that it is the latter that determines the former.

Variation of Solar Rotation with Latitudes

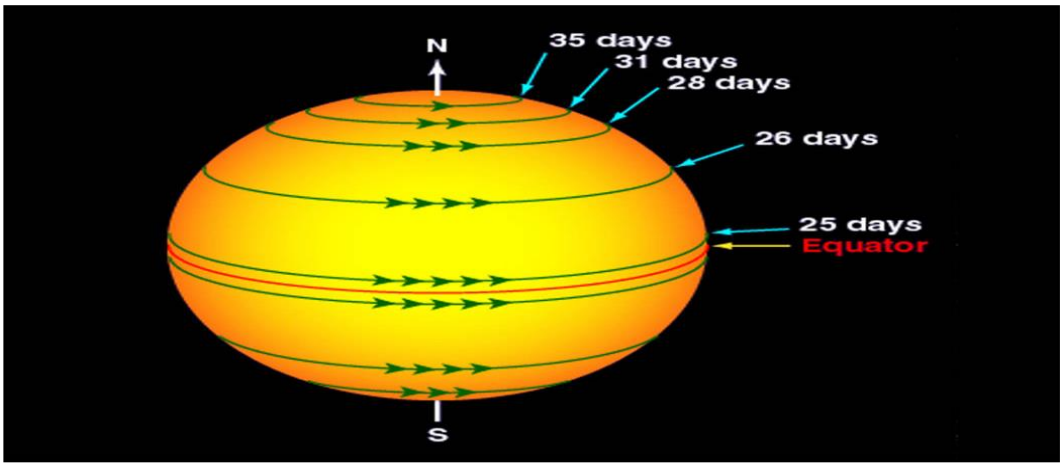

Courtesy: from NASA website

Figure 9: The Rotational Rate of the Sun at Different Latitudes

Right after the telescope was created, in or around 1610, the Solar rotation was identified. On the sun's surface, which rotates differently, Carrington developed a physically singular way to define longitude. In order to represent this, Carrington suggested a notation that divided time in to intervals of 27.27 days. On November 9, 1853, the term "rotation" was first used. Sun, a ball of gas and plasma, is not a physical entity. Thus, it rotates at a different rate than other solids like the Earth seen in Figure (9). The regions close to the sun's equator revolve every 25 days. The Sun rotates more slowly at the poles because its rotational speed decreases with increasing latitude. The Sun spins for 36 days while it is at its poles. While the Sun's surface spins in a similar manner, its interior does not. The "tachocline" marks the separation between the Sun's inner, continuously spinning components and its outer, irregularly spinning components.

Convection currents convey the charged plasma from deep within the Sun to the surface of the Sun, and together with differential rotation of the outer layers, they have a

significant impact on the Sun's magnetic field behaviour. According to observations, differential rotation is the primary cause of the 11-year sunspot cycle and the related 22-year solar cycle. In 1961, American astronomer Horace Babcock proposed the Babcock Model, so named after his idea that differential rotation and convective motion cause these cycles.

X. SOLAR ACTIVITY AND ITS PARAMETERS

1. **Sunspot regions:** Hale was the first to discover that the Sun's magnetic field is extremely convoluted in both space and time in 1908. Because sun spots have a lower temperature than their surroundings, they appear darker on the surface (Kirchhoff's emission law). Sunspots are areas of decreased brightness in the photosphere, or the surface layer of the Sun, that are connected with strong magnetic fields. They are assumed to be manifestations of an inner magnetic dynamo, and they are associated with atmospheric activity such as flaring and coronal mass ejections. A sunspot is an intense magnetic flux tube that emerges from the convection zone of the photosphere. Parker explained the magnetic field of a sunspot emanating from one spot and returning to another in 1955, owing to the fact that sunspots generally develop in larger groups or pairs. Sunspots and the magnetic field are intricately related. The low temperature causes the high magnetic field of sunspots, and overall pressure and magnetic energy density must be balanced. The greatest sunspot has a maximum diameter of around 20000 kilometres. The umbra is the centre of the spot (whose temperature is around 4100 deg K and magnetic field is around 0.3 T) and the penumbra, which comprises of dark and bright filaments, is seen in Figure (10). Around 2,800, years ago, Chinese astronomers made the first recorded-observation of sunspots [19].

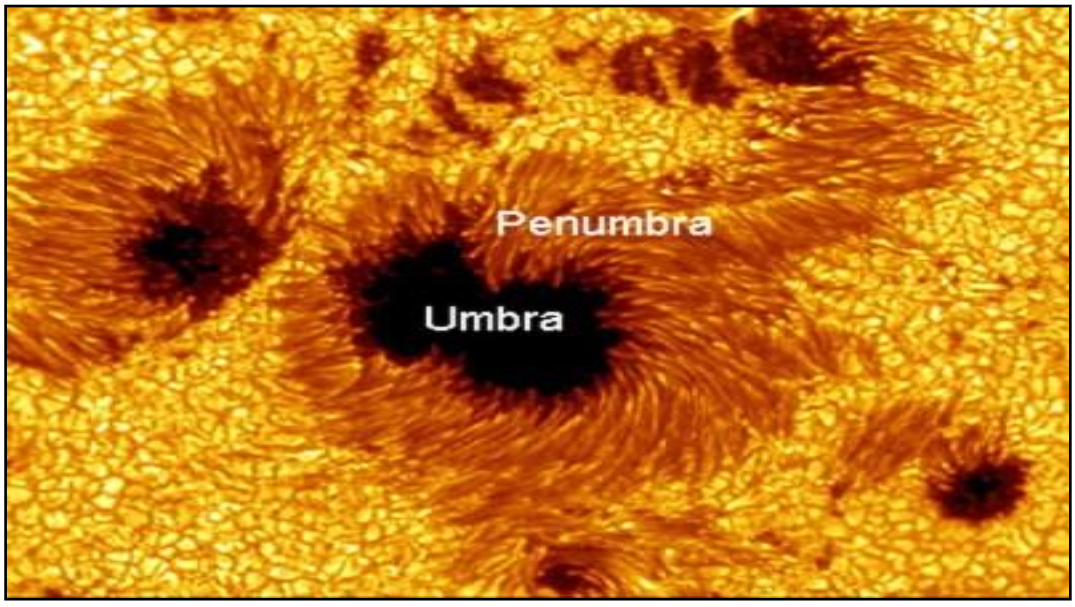

Courtesy: from NASA website

Figure 10: An Image of a Sunspot and Solar Granulation Obtained from Hinode Spacecraft.

2. **Solar radio flux (F10.7 cm):** Solar Radio Flux (F10.7 cm) is the Sun's disc-integrated 2800 MHz emission [20]. The Canadian Solar Radio Monitoring Programme has measured this flow since 1946. Several measures are taken daily to avoid flaring-influenced readings. From 1946 through 1990, Ottawa was observed. In 1990, a second flux monitor, located in Penticton, British Columbia, was installed to serve as a backup to the primary monitor in Ottawa. Covington's F10.7 Solar radio flux is a typical measure of solar activity [17]. It is the density of microwave radiation at 10.7 cm in wavelength for |B| = 103 G. Japan quickly established routine observations at four predetermined frequencies (1.0, 2.0, 3.75, and 9.4 GHz) spanning the F10.7 (2.8 GHz) and included Solar gyro resonance signature shortly after its introduction. [21] used these data to create a microwave photometric standard.

   The National Research Council of Canada was established in 1947 and has measured solar F10.7 radiation at 2800 MHz (10.7cm wavelength) (NRCC). Observations were done at Algonquin Radio Observatory till May 31, 1991. The Dominion Radio Astrophysical Observatory in Penticton, British Columbia, is home to the Solar Radio Monitoring Programme, which has made its measurements of the Sun's radio flux F10.7 from 1990 to 1991 available online at http://www.ngdc.noaa.gov/stp/space-weather/.

3. **Solar wind plasma:** Solar Wind is the name given to the process through which the Sun's gravitational pull is lost to space. It is present in the form of magnetised plasma and predominates in the Sun's heliosphere. In 1958, E. Parker made a prediction about the Solar wind, and in 1962, he validated its existence. It has been observed mostly on the ecliptic plane, but also at both polar poles; its closest approach to the Sun was 0.29 astronomical units, while its furthest separation from the Sun was 70 astronomical units. The fundamental properties of the solar wind change dramatically depending on where one is in relation to the Earth's orbit. A phenomenon known as solar wind is what creates the connection between the atmosphere of the sun and our own. Solar wind can have different densities, velocities, temperatures, and magnetic fields depending on factors such as the solar cycle, heliographic latitude, heliocentric distance, and rotation period. Alterations are caused when shocks, waves, and turbulences are transferred from one planet to another.

   Slow solar wind (400 km/s) is produced by closed magnetic fields, and fast solar wind (600-800 km/s) is produced by coronal holes. During Solar Maximum, coronal holes congregate around the equator. On the inactive Sun, fast solar wind arises through magnetically open coronal holes. High-speed solar wind is a distinct type. The heliosphere is fully blanketed by solar wind, which arises from large coronal holes at latitudes over 400-600. The Sun's active regions are where the minimum solar wind is produced. It encompasses the heliospheric current sheet and is restricted to the warped streamer belt. Low helium content in this solar wind suggests a greater release height.Large solar eruptions produce plasma clouds with high helium percentages (30%) and other characteristics.

4. **Interplanetary Magnetic Field (IMF):** Bx, By, and Bz are the three components of the IMF's vector form, with Bx and By parallel to the ecliptic and Bz perpendicular to it. It is caused by solar wind waves or other types of disturbances. When the IMF and geomagnetic field lines are antiparallel to each other, energy, mass, and momentum can

be transmitted from the solar wind to the magnetosphere. The Bz component with a southerly orientation pairs the strongest and has the most influence on the magnetosphere. The IMF is a component of the Sun's magnetic field that is transported into interplanetary space by the Solar wind because its field lines are frozen in the plasma of the Solar wind. Because the Sun spins, solar wind sweeps out from the star in a spiralling pattern. The strength of the IMF field around Earth ranges from 1 to 37 nT, with an average of 5 nT.

5. **Geomagnetic storms:** Space weather is defined by geomagnetic storms [21-23]. Extreme solar storms can have a negative impact on technology [24, 25]. At http://swdcwww.kugi.kyoto-u.ac.jp/, the Dst index evaluates geomagnetic storm strength. Nonlinear geomagnetic storms and substorms exist. Previous research has shown geomagnetic time series self-affinity [26,27,29,30]. Variations in the external geomagnetic field exhibit a varying power law spectrum. Geomagnetic field at several scales [31, 29]. Long-lasting perturbations in the geomagnetosphere are known as geomagnetic storms [29]. Classical techniques, such as the Fourier Transform for analysing the geomagnetic index Dst, cannot provide information on the temporal course of geomagnetic storms. When the aurora intensifies and extends to low magnetic latitudes, the magnetosphere generates energetic charge particles. D, Z, and H are measurements of the earth's magnetic field. (H). Dst index was produced by Sugiura (1964).

   A geomagnetic storm has an onset, peak, and recovery period. Isolated geomagnetic storms are used in the research. Loewe's Dstmin [32] is shown in Table 1.

Table 1 : Classification of Geomagnetic Storm Intensity

Storm Type	***Weak***	***Moderate***	***Strong***	***Severe***	***Great***
Dst_{min} range in nT	-50~-30	-100~-50	-200~-100	-350~-200	≤-350

6. **Space Plasmas and Magnetohydrodynamics (MHD):** MHD considers space plasmas electrically conductive fluids. It has been effectively applied to heliosphere space plasma research to analyze the "macroscopic picture of various solar plasma events" using conductivity fluid equation and numerical modeling and simulation.

7. **Magneto-hydro-dynamic (MHD) waves:** Magneto hydrodynamic (MHD) waves can be discovered in many different types of space plasma. By restoring magnetic and thermal forces in the solar wind, these MHD waves are created. The local magnetic field, which is perpendicular to the field lines, does not compress alfven waves, which are transverse waves that cause changes in plasma in the solar wind. The determination of MHD waves in space plasma is typically done indirectly, by comparing the corresponding properties like propagation speed or variation in pressure, as well as with theoretically derived properties, as opposed to the magnetosphere and solar wind, which provide direct in situ measurements. It has been difficult to detect MHD waves because space plasmas are frequently highly inhomogeneous as a result of magnetism, changes in plasma density and temperature, or plasma flows. Due to the difficulties this significant inhomogeneity poses for comprehending magnetohydrodynamic wave occurrences, magnetic flux tubes and plasma flow tubes are of particular significance. Oscillatory events have been seen in

sunspots, solar photospheric magnetic flux tubes, coronal loops, and polar plumes, among other forms of flux tube structures in the solar environment. Both solar flares and prominences on the sun oscillate.

XI. METHODS OF ANALYSIS

A great variety of non-linear techniques based on wavelets and cross-recurrence plots (CRPs) have been used for these parameters of sunspots, solar radio flux (F10.7cm flux), plasma properties in solar wind, strength of interplanetary magnetic field (IMF), and so on are just some of the solar activity indices that can be analyzed.

1. **Wavelet transform:** The spectral features of a time series are estimated through wavelet analysis as a function of time to show how the various periodic components of the time series change with time. It is appropriate to analyse events with non-stationary power and time series with erratic distributions at a variety of frequencies. The ability of the wavelet transform to do organic local analysis of a time series is a key advantage. The wavelet expands into a long function to capture low-frequency motions while condensing into a short function to capture high-frequency motions. Many works by [33–40] rely on discretized wavelet transforms (DWT).

   Data compression, nuclear engineering, sub-band coding, signal and image processing, neurophysiology, music, magnetic resonance imaging, speech discrimination, optics, fractals, radar, human vision, pure mathematics, and geophysics (e.g., tropical convection, the El Nino-Southern Oscillation, atmospheric cold fronts, temperature variability, the dispersion of ocean waves, wave growth, and breeziness) are all applied [35–37].

2. **Discrete Wavelet Transform (DWT):** In the discrete wavelet transform (DWT), the location and scale of a signal are often determined dynamically [38]. Signal and noise separation works quite well with the DWT [39]. The dimension-wise transformation (DWT) of a vector creates a new vector with the same dimensions as the original vector [45]. The decomposition procedure is this transformation. In this study, all time series (for all Solar Cycles 20–24) were divided using the Duabechies and Coifman wavelets. In addition to providing compact support, the Daubechies wavelet also shows complete scaling, translational orthonormality, and non-zero basis functions over a finite duration [42]. These characteristics are crucial for pinpointing the precise location of occurrences in time-dependent signals [43]. Time series can be broken down into their approximate and exact parts using DWT.

3. **Continuous Wavelet Transform (CWT):** The continuous wavelet transform (CWT) produces a frequency spectrum from a time series that is simply a function of one dimension, which contains a lot of redundant information. Increasing numbers of scientists are turning to CWTs in their investigations [44-49] Explain how these methods have been put to good use in the economic realm.

4. **Cross Wavelet Transform (XWT):** Using the cross wavelet transform (XWT), wavelet transformations can be expanded to display the common power and relative phase in

time-frequency space between two time series [50]. The cross wavelet transform of the two time series X and Y is defined as

$$W^{XY} = W^{X}W^{Y*}, \qquad \ldots\ldots\ldots\ldots (1)$$

Where W^X and W^Y are the continuous wavelet transformations, and * signifies complex conjugation [51]. The time-frequency space representation of the complex argument arg (W^{XY}) can be thought of as a local relative phase between X and Y. High common power is revealed by calculating cross-wavelet power.

5. **Wavelet Coherence Transform (WTC):** The wavelet coherence (WTC) is an estimator of the confidence level for the discovery of a time-space region with high common power and consistent phase connection. It is produced when the cross wavelet transform between two time series is applied. In time-frequency space, it is most analogous to a localised correlation coefficient and can take on values ranging from 0 to 1. The measure of wavelet coherence is defined between two continuous wavelet transformations. It is possible for this measure to suggest coherence with a high confidence level even when the shared power is low.

6. **Cross Recurrence Plots (CRPs):** Researchers are able to study the temporal correlations between two processes that are both represented in a single time series by using an extension of recurrence plots called CRPs [52-54]. These plots are called CRPs. In order to understand how these processes are related, this method compares their phase space trajectories.

7. **Multifractal analysis:** To distinguish between a rough or broken geometric structure that demonstrates a high degree of self-similarity within its own fractional dimensions, fractals were first found by [55]. Recent research on fractal patterns has focused on physics and commerce, among other areas. R&S analysis for hydrological investigations was first introduced in [56]. The detrended fluctuation analysis (DFA) technique for DNA sequence analysis was developed by [57] to meet this challenge. The multiscale and fractal subsets of the time series cannot be described using DFA, despite the fact that it has become a popular method for discovering monofractal scaling properties. [58] expanded the DFA to multifractal detrended fluctuation analysis for the goal of multifractal characterization of non-stationary time series (MFDFA). The MFDFA has been used to analyse a variety of topics, including international crude oil markets [59], foreign exchange markets [60], stock markets [61], gold markets [62], and agricultural commodity futures markets [73]. Researchers generalising DFA and MF-DFA analysis by focusing on detrended covariance explored cross-correlations between two non-stationary time series [64–67].

XII. CONCLUSION

In order to carry out a study of the astronomical and solar data, one can make use of a large variety of one-of-a-kind mathematical transformations. The Fourier transform is one of these procedures that is utilised frequently and is also comprehended by its users. The Wavelet Transform is utilised in circumstances where a higher level of performance is sought in order to circumvent the limitations that it imposes on the system. This is done since the

Wavelet Transform has some restrictions of its own. On the other hand, the ability to localize both time and frequency enables it to concurrently turn a one-dimensional time series into a diffuse two-dimensional time-frequency image. This enables it to break down or alter the series. The wavelet that is employed in the wavelet analysis will always have the same form; the only thing that will change is the size of the wavelet, which will vary depending on the size of the window. Learning the phase of any periodic signals is helpful and should be done in addition to mastering the amplitude of those signals. This chapter has brought to our attention the wavelet technique, which has been put to use in the past to analyse the properties of the solar wind and locate periodic changes that could be the cause of geomagnetic disturbances. Wavelet spectrum analysis gives a logical basis for estimating the time-frequency properties of the data that has been investigated. During wavelet analysis of signals, the level fluctuation of solar wind parameters is mapped into a variety of scales and temporal instants using a Morlet wavelet function.

REFERENCES

[1] Tsurutani Bruce T., Gonzalez, W.D.: The efficiency of 'viscous interaction' between the solar wind and the magnetosphere during intense northward IMF events, Geophysical Research Letters (ISSN 0094-8276), 22, 6, 663-666, 1995.
[2] Gopalswamy, Nat.: Halo coronal mass ejections and geomagnetic storms, Earth, Planets and Space, 61, 595-597, 2009.
[3] Temmer, M., Veronig, A., & Hanslmeier, A. 2002, A&A, 390, 707.
[4] Bogart R.S.: Recurrence of solar activity: Evidence for active longitudes, *Sol. Phys.* 76,155, 1982.
[5] Veronig , A, Messerotti, M., Hanslmeier, A.: Determination of fractal dimensions of solar radio bursts, *Astron. Astrophys.*
[6] Jevtic, N., Schweitzer. J.S., Cellucci, C.J.: Nonlinear time series analysis of northern and southern solar hemisphere daily sunspot numbers in search of short-term chaotic behavio, *Astron. Astrophys.*, 379, 611 - 615, 2001.
[7] Abramneko, V.I., Longcope, D.W.: Distribution of the Magnetic Flux in Elements of the Magnetic Field in Active Regions, *The Astrophysical Journal*, 619, 2,1160-1166, 2005.
[8] Movahed, M.S., Jafari, G.R., Ghasemi, F., Rahvar. S., Tabar, M.R.R.: Multifractal detrended fluctuation analysis of sunspot time series, *J. Stat. Mech.*, P02003, 2006.
[9] McAteer R.T.J., Young, C.A., Ireland, J. Gallagher, P.T.: The Bursty Nature of Solar Flare X-Ray Emission , *Astrophys. J.*, 662 (1), 691 - 700, 2007.
[10] Bruevich, E.A., Yakunina, G.V.: The study of time series of monthly averaged values of F10.7 from 1950 to 2010, *Sun and Geosphere*, 7 (1), 65 - 70, 2012.
[11] Zririn, H.: Book-Review - Astrophysics of the Sun, KNUDSEN, Science, 242, 4885/DEC16, 1586, 1988
[12] Vassenius, B.: Observatio Eclipsis Solis Totalis Cum Mora Facta Gothoburgi Sveciae, Sub Elev. *Trans. Roy. Soc. London*, 38, 134 – 135, 1733.
[13] Galsgaard, K., Longbottom, A.W.: Formation of Solar Prominences by Flux Convergence, *ApJ*, 510, 444 - 459, 1999.
[14] Leroy J.L, Bommier, V., Sahal-Brechot, S., Solar Phys, 83, 135, 1983
[15] Schwabe, M.: Sonnenbeobachtungen im Jahre 1843. Von Herrn Hofrath Schwabe in Dessau, *Astronomische Nachrichten*, 21, 233, 1844.
[16] Clark D.H., Stephenson F.R.: An interpretation of the pre-telescopic sunspot records from the orient, *Q.J. Roy. Astron. Soc*. 19, 387 - 410, 1978.
[17] Tapping, K.F., Charrios, D.P.: Limits of the accuracy of the 10.7 CM flux, Solar Physics, vol. 150, no. 1-2, p. 305-315, 1994.

[18] Tanaka, H., Castelli, J.P., Covington, A. E., Kruger, A., Landecker, T. L., Tlamicha, A.: Absolute calibration of solar flux density in the microwave region, *Sol. Phys.*, 29, 243 – 262, 1973.
[19] Kamide, Y., Yokoyama, N., Gonzalez, W.D., Tsurutani, B.T., Daglis, I.A., Brekke, A., Masuda, S.: Two-step development of geomagnetic storms, *J. Geophys. Res*.,103, 6917 - 6921, 1998a.
[20] Freeman, J.W.: Storms in Space, *Cambridge University Press*, 2001.
[21] Angelopoulos, V.: The THEMIS Mission, *Space Science Reviews*, 141 (5), 1 - 4, 2008.
[22] Baker, D.N.: The occurrence of operational anomalies in spacecraft and their relationship to space weather, *IEEE Trans. Plasma Sci.*, 28 (6), 2007 - 2016, 2000.
[23] Daglis, I.A., Baker, D.N., Galperin, Y., Kappenman, J.G., Lanzerotti, L.J.: Tchonological imapacts of space storms: Outstanding issues, Eos, Transactions American Geophysical Union, Volume 82, Issue 48, p. 585-585, 2001.
[24] Balasis, G., Daglis, I., Kapiris, P., Mandea, M., Vassiliadis, D., Eftaxias, K.: From pre-storm activity to magnetic storms: A transition described in terms of fractal dynamics, *Ann. Geophys.*, 24, 3557 - 3567, 2006.
[25] Uritsky, V.M., Klimas, A.J., Vassiliadis, D.: Comparative study of dynamical critical scaling in the auroralelectrojet index versus solar wind fluctuations, *Geophys. Res. Lett.*, 28, 3809 - 3812, 2001.
[26] Loewe, C.A., Prolss, G.W.: Classification and mean behavior of magnetic storms, *J. Geophys. Res*., 102, 14209 - 14213, 1997.
[27] Ramsey, J.B., Lampart, D.C.: Decomposition of Economic Relationship by Time Scales Using Wavelets, *Macroeconomic Dynamics*, 2(1), 49 – 71, 1998a.
[28] Ramsey, J.B., Lampart, D.C.: The Decomposition of Economic Relationship by Time Scale Using Wavelets: Expenditure and Income, *Studies in Nonlinear Dynamics and Econometrics*, 3 (1), 23 – 42, 1998b.
[29] Ramsey,J.B.: The contribution of wavelets to the analysis of economic and financial data, Phil. *Trans. R. Soc.Lond.A*, 357, 2593 – 2606, 1999; reprinted in Wavelets, edt. Silverman, B.W., Vassilicos, J.C.: *Oxford Univ. Press, Oxford*, Chapter 12, 221 - 236, 1999.
[30] Ramsay, J.O., Ramsey, J.B.: Functional data analysis of the dynamics of the monthly index of nondurable goods production, *Journ. of Econometrics*, 107, 327 - 344, 2002.
[31] Gencay, R., Selcuk, F., Whitcher, B.: Scaling properties of foreign exchange volatility, *Physica A*, 289, 249 - 266, 2001a.
[32] Gencay, R., Selcuk, F., Whitcher, B.: Multiscale Systematic Risk, *Journal of International Money and Finance*, 24(1), 55 - 70, 2005.
[33] Connor, J., Rossiter, R. Wavelet Transforms and Commodity Prices, *Studies in Nonlinear Dynamics & Econometrics*, 9 (1). 6, 20, 2005.
[34] Gallegati, M., Gallegati, M.: Wavelet variance analysis of output in g-7 countries', *Studies in Nonlinear Dynamics & Econometrics*, 11(3), 2007.
[35] Farge, M.: Wavelet transforms and their applications to turbulence, *Ann. Rev. Fluid Mech.* 24, 395 – 457, 1992.
[36] Graps, A.: An introduction to wavelets, *IEEE Comp. Sci. Engng*, 2 (2), 50 – 61, 1995.
[37] Torrence, C., Compo, G.P.: A practical guide to wavelet analysis, *Bull. Am. Meteorol. Soc*., 79, 61 - 78, 1998.
[38] Chou, C.M.: Applying multi resolution analysis to differential hydrological grey models with dual series. *J. Hydrol*. 332 (1 - 2), 174 – 186, 2007.
[39] Fugal, D.L.: Conceptual wavelets in Digital Signal Processing. An in-depth, Practical Approach for the Non-mathematician, *first ed. Space & Signals Technologies LLC*, 2009.
[40] Chou, C.M.: Wavelet-based multi-cscale entropy analysis of complex rainfall time series. *Entropy*, 13 (1), 241 – 253, 2011.
[41] Vonesch, C., Blu, T., Unser, M.: Generalized Daubechies Wavelet families, *IEEE Trans. Signal Process*, 55 (9), 4415 – 4429, 2007.

[42] Popivanov, I., Miller, R.J.: Similarity search over time-series data using wavelets, *In Proceedings of the 18th International Conference on Data Engineering (ICDE)*, 2002.
[43] Popivanov, I., Miller, R.J.: Similarity search over time-series data using wavelets, *In Proceedings of the 18th International Conference on Data Engineering (ICDE)*, 2002.
[44] Raihan, Wen, Zeng.: Wavelet: a new tool for business cycle analysis, *Working paper 2005 - 050 A, Fedral Reserve Bank of St. Louis*, 2005.
[45] Crowley, P., Mayes, D.: How fused is the euro area core? An evaluation of growth cycle co movement and synchronization using wavelet analysis, *Journal of Business Cycle Measurement and Analysis*, 4, 63 - 95, 2008.
[46] Aguiar-Conraria, L., Azevedo, N., Soares, M.J.: Using Wavelets to Decompose the Time-Frequency Effects of Monetary Policy, *Physica A: Statistical Mechanics and its Applications*, 387, 2863 - 2878, 2008.
[47] Baubeau, P., Cazelles, B.: French economic cycles: a wavelet analysis of French retro-spective GNP series, *Cliometrica* 3, 275 – 300, 2009.
[48] Rua, A., Nunes, L.C.: International co-movement of stock market returns: A wavelet analysis, *Journal of Empirical Finance* 16, 632 – 639, 2009.
[49] Rua, A.: Measuring co-movement in the time - frequency space, *Journal of macroeconomics 32*, 685 – 691, 2010.
[50] Li, X., Yao, X., Jefferys, J.G.R., Fox. J.: Computational neuronal oscillation with morlet wavelet transform, *Proceedings of 27th annual international conference of the IEEE engineering in medicine and biology Society, Shanghai, SEP., IEEE Press*, 1 - 4, 2005.
[51] Grinsted, A., Moore, J.C., Jevrejeva, S.: Application of the cross wavelet transform and wavelet coherence to geophysical time series, *Nonlinear Proc Geophys*,11, 561 – 566, 2004.
[52] Zbilut, J.P., Giuliani, A., Webber Jr., C.L.: Detecting deterministic signals in exceptionally noisy environments using cross-recurrence quantification, *Physics Letters*, A 246 (1-2), 122 – 128, 1998. M
[53] Marwan, N., Kurths, J.: Nonlinear analysis of bivariate data with cross recurrence plots, *Physics letters A*, 302, 299 - 307, 2002.
[54] Marwan, N., Thiel, M., Nowaczyk, N.R.: Cross recurrence plot based synchronization of time series, *Nonlin. Processes Geophys*., 9, 325 - 331, 2002a.
[55] Mandelbrot, B.: The Fractal Geometry of Nature, *Freeman, New York*, 1983.
[56] Hurst, H.: Long term storage capacity of reservoirs, *Transactions of the American Society of Engineers*, 116, 770 – 799, 1951.
[57] Peng, C.K., Buldyrev, S.V., Havlin, S., Simons, M., Stanley, H.E., Goldberger, A.L.: Mosaic organization of DNA nucleotides, *Phys. Rev. E* 49, 1685 - 1689, 1994.
[58] Kantelhardt, J.W., Zschiegner, S.A., Kosciilny-Bunde, E., Havlin,S., Bunde, A., Stanley, H.E.: Multifractal detrended fluctuation analysis of nonstationary time series, *Physica A: Statistical Mechanics and its Applications*, 316, 1, 87 - 114, 2002.
[59] Gu, R.B., Chen, H.T., Wang, Y.D.: Multifractal analysis on international crude oil markets based on the multifractal detrended fluctuation analysis, *Physica A* 389, 2805 – 2815, 2010.
[60] Norouzzadeh, P., Rahmani, B.: A multifractal detrended fluctuation description of Iranian rialUS dollar exchange rate, *Physica A*, 367, 328 – 337, 2006.
[61] Yuan, Y., Zhuang, X.T., Jin, X.: Measuring multifractality of stock price fluctuation using multifractal detrended fluctuation analysis, *Physica A*, 388, 2189 - 2197, 2009.
[62] Wang, Y.D., Liu, L.: Is WTI crude oil market becoming weakly effi- cient over time? New evidence from multiscale analysis based on detrended fluctuation analysis. *Energy Economics 32*, 987 – 992, 2010.
[63] Li, Z., Lu, X.: Multifractal analysis of China's agricultural commodity futures markets, *Energy Procedia*, 5, 1920 – 1926, 2011.
[64] Podobnik, B., Stanley, H.E.: Detrended cross-correlation analysis: a new method for analyzing two nonstationary time series, *Physical Review Letters,100*, 084102, 2008.

[65] Podobnik, B., Horvatic, D., Petersen, A.M., Stanley, H.E.: Cross-correlations between volume change and price change, *Proceedings of the National Academy of Sciences of the United States of America 106,* 22079 – 22084, 2009.
[66] Zhou, Wei-Xing.: Multifractal detrended cross-correlation analysis for two non-stationary signals, Physical Review E, 77, 6, 2008.
[67] Li, Z., Lu, X.: Cross-correlations between agricultural commodity futures markets in the US and China, *Physica A*, 391, 3930 – 3941, 2012.

